Numerical Simulations of the Formation of Hurricane Gabrielle (2001)

K. D. MUSGRAVE

Department of Atmospheric Science, Colorado State University, Fort Collins, Colorado

C. A. DAVIS

National Center for Atmospheric Research, Boulder, Colorado*

M. T. MONTGOMERY

Department of Meteorology, Naval Postgraduate School, Monterey, California

(Manuscript received 5 December 2006, in final form 25 June 2007)

ABSTRACT

This study examines the formation of Hurricane Gabrielle (2001), focusing on whether an initial disturbance and vertical wind shear were favorable for development. This examination is performed by running numerical experiments using the fifth-generation Pennsylvania State University–National Center for Atmospheric Research Mesoscale Model (MM5). Gabrielle is chosen as an interesting case to study since it formed in the subtropics only a few days before making landfall in Florida. Three simulations are run: a control run and two sensitivity experiments. The control run is compared with observations to establish the closeness of the model output to Gabrielle's observed formation. The two sensitivity experiments are designed to test the response of the developing tropical cyclone to alterations in the initial conditions. The first sensitivity experiment removes the initial (or precursor) disturbance, a midtropospheric vortex located over Florida. The second sensitivity experiment reduces the vertical wind shear over the area of formation. The control run produces a system comparable to Gabrielle. The convection in the control run is consistently located downshear of the center of circulation. In the first sensitivity experiment, with the removal of the initial disturbance, no organized system develops. This indicates the importance of the midtropospheric vortex in Gabrielle's formation. The second sensitivity experiment, which reduces the vertical wind shear over the area of Gabrielle's formation, produces a system that can be identified as Gabrielle. This system, however, is weaker than both the control run and the observations of Gabrielle. This study provides direct evidence of a favorable influence of modest vertical wind shear on the formation of a tropical cyclone in this case.

1. Introduction

Over the past half-century, research in the area of tropical cyclogenesis has established several factors believed to be necessary for tropical cyclone formation (Gray 1968; Riehl 1948; Palmen 1948). These factors include such things as sea surface temperatures greater than approximately 26°C, upper-tropospheric divergence, a moist lower to middle troposphere, a preexisting cyclonic disturbance, and an absence of significant vertical wind shear. While the definition of "significant" is not universally agreed upon, the threshold is usually defined as a velocity difference somewhere in the range of 10–15 m s^{-1} in the 850–200-hPa layer (DeMaria et al. 2001; Bracken and Bosart 2000).

A significant amount of deep tropospheric vertical wind shear is generally believed to be detrimental to the formation of tropical cyclones, but whether vertical wind shear is always detrimental is currently under debate. Bracken and Bosart (2000) suggested the possibility that a small amount of vertical wind shear is necessary for development to help to force synoptic-scale ascent, as opposed to the idea that minimal or zero vertical wind shear is optimal (Gray 1968; McBride and Zehr 1981). In storm-centered composites covering roughly 3000 km × 3000 km they found an average

* The National Center for Atmospheric Research is sponsored by the National Science Foundation.

Corresponding author address: K. D. Musgrave, Department of Atmospheric Science, Colorado State University, Fort Collins, CO 80523.
E-mail: kate@atmos.coostate.edu

DOI: 10.1175/2007MWR2110.1

Report Documentation Page

Form Approved
OMB No. 0704-0188

1. REPORT DATE	2. REPORT TYPE	3. DATES COVERED
JUN 2007		**00-00-2007 to 00-00-2007**

4. TITLE AND SUBTITLE	5a. CONTRACT NUMBER
Numerical Simulations of the Formation of Hurricane Gabrielle (2001)	5b. GRANT NUMBER
	5c. PROGRAM ELEMENT NUMBER
6. AUTHOR(S)	5d. PROJECT NUMBER
	5e. TASK NUMBER
	5f. WORK UNIT NUMBER
7. PERFORMING ORGANIZATION NAME(S) AND ADDRESS(ES) **Naval Postgraduate School,Department of Meteorology,Monterey,CA,93943**	8. PERFORMING ORGANIZATION REPORT NUMBER
9. SPONSORING/MONITORING AGENCY NAME(S) AND ADDRESS(ES)	10. SPONSOR/MONITOR'S ACRONYM(S)
	11. SPONSOR/MONITOR'S REPORT NUMBER(S)

12. DISTRIBUTION/AVAILABILITY STATEMENT

Approved for public release; distribution unlimited

13. SUPPLEMENTARY NOTES

14. ABSTRACT

This study examines the formation of Hurricane Gabrielle (2001), focusing on whether an initial disturbance and vertical wind shear were favorable for development. This examination is performed by running numerical experiments using the fifth-generation Pennsylvania State University?National Center for Atmospheric Research Mesoscale Model (MM5). Gabrielle is chosen as an interesting case to study since it formed in the subtropics only a few days before making landfall in Florida. Three simulations are run: a control run and two sensitivity experiments. The control run is compared with observations to establish the closeness of the model output to Gabrielle?s observed formation. The two sensitivity experiments are designed to test the response of the developing tropical cyclone to alterations in the initial conditions. The first sensitivity experiment removes the initial (or precursor) disturbance, a midtropospheric vortex located over Florida. The second sensitivity experiment reduces the vertical wind shear over the area of formation. The control run produces a system comparable to Gabrielle. The convection in the control run is consistently located downshear of the center of circulation. In the first sensitivity experiment, with the removal of the initial disturbance, no organized system develops. This indicates the importance of the midtropospheric vortex in Gabrielle?s formation. The second sensitivity experiment, which reduces the vertical wind shear over the area of Gabrielle?s formation, produces a system that can be identified as Gabrielle. This system, however, is weaker than both the control run and the observations of Gabrielle. This study provides direct evidence of a favorable influence of modest vertical wind shear on the formation of a tropical cyclone in this case.

15. SUBJECT TERMS

16. SECURITY CLASSIFICATION OF:			17. LIMITATION OF ABSTRACT	18. NUMBER OF PAGES	19a. NAME OF RESPONSIBLE PERSON
a. REPORT **unclassified**	b. ABSTRACT **unclassified**	c. THIS PAGE **unclassified**	**Same as Report (SAR)**	**17**	

Standard Form 298 (Rev. 8-98)
Prescribed by ANSI Std Z39-18

vertical wind shear of about 10.5 m s^{-1} in the 900–200-hPa layer. Davis and Bosart (2003) list several cases in the 2000 and 2001 Atlantic hurricane seasons where vertical wind shear ranged between 12 and 14 m s^{-1}, and three cases in which initial vertical wind shear reached or exceeded 30 m s^{-1} during formation.

The debate regarding vertical wind shear in observational studies of tropical cyclones carries over into theoretical studies. Vertical wind shear is believed to play several different roles in the formation of a tropical cyclone. Some of these roles are detrimental to the formation of a tropical cyclone, while some are beneficial, and some are not so clear. In cases with lower- to mid-tropospheric vortex precursors to genesis, vertical wind shear can deform the vertical structure of the vortex, displacing deep convection away from the low-level center. While this often destroys the developing system, Montgomery and Kallenbach (1997) proposed that convection displaced from the center causes vorticity asymmetries, which may axisymmetrize into the developing vortex and accelerate the mean tangential winds. With sustained deep convective activity, this represents a possible mechanism for tropical cyclone formation (Montgomery and Enagonio 1998). In this case the determination of whether vertical wind shear is a positive or negative influence on formation is dependent on how far the convection is displaced from the center.

Another way that vertical shear may affect tropical cyclone formation is through its influence on the precursor disturbance that forms the seed of the developing tropical cyclone. Precursor disturbances range from easterly waves (Reed et al. 1977) to monsoon troughs (Gray 1968) to baroclinic systems (Bosart and Bartlo 1991; Davis and Bosart 2001, 2003). Baroclinic systems cover a range of disturbances in both the mid- and upper troposphere, whose upward motion can be influenced by vertical wind shear, including tropical upper-tropospheric troughs (TUTTs) and mesoscale convective vortices (MCVs). Riehl (1948), among others, has linked TUTTs to tropical cyclogenesis (Sadler 1976; Bracken and Bosart 2000). Several studies have suggested MCVs as precursor disturbances. Some theories for the formation of tropical cyclones involve the transformation of one (Bister and Emanuel 1997) or self-aggregation of several MCVs (Simpson et al. 1997; Ritchie and Holland 1997) and top-down development into a single surface-concentrated vortex. Another theory suggests tropical cyclone formation from an initial MCV through bottom-up development (Montgomery and Enagonio 1998; Möller and Montgomery 2000; Montgomery et al. 2006).

MCVs are thought to form in the stratiform region of mesoscale convective systems (MCSs); they are believed to be important because they typically outlive the convection that spawns them and can retrigger subsequent convection, which can then reinvigorate the vortex (Raymond and Jiang 1990, hereinafter RJ90). MCVs tend to be on the scale of tens to hundreds of kilometers in the horizontal, and located about 2–6 km above ground level (Trier et al. 2000a). MCVs have been studied extensively for their role in continental convection (e.g., RJ90; Trier et al. 2000a,b; Trier and Davis 2002; Davis and Trier 2002).

One way of understanding the formation and life cycle of an MCV is to adopt a potential vorticity (PV) framework. RJ90 laid the groundwork for PV thinking on the mesoscale. They use a nonlinear balance model to explain the basics of an MCV life cycle. The convection associated with an MCS removes mass (within isentropic layers) from the lower troposphere and deposits the mass in the upper troposphere. The removal of mass in the lower troposphere concentrates PV in those isentropic layers, and the addition of mass in the upper troposphere dilutes PV (Haynes and McIntyre 1987; Raymond 1992). This process leads to a lower-level positive (cyclonic) PV anomaly and an upper-level negative (anticyclonic) PV anomaly. The vertical radius of influence of the PV anomalies extends only a few kilometers due to the limited horizontal extent of MCSs. For this reason the upper negative PV anomaly can be neglected when considering the effects on future convection, leaving only the lower positive PV anomaly (the MCV) to effect future convection. In the absence of diabatic effects a positive PV anomaly in the presence of linear vertical shear produces upward motion on its downshear side (RJ90; Trier et al. 2000a; Raymond 1992). Three distinct factors contribute to upward motion downshear of the positive PV anomaly: the background flow along isentropes perturbed by the vortex, the vortex circulation upgliding and downgliding along isentropes in thermal wind balance with the background flow, and the tilt of the vortex.

The upward motion that results from an MCV interacting with vertical shear, in combination with other environmental factors, can be sufficient to trigger new convection downshear of the MCV. Trier et al. (2000a) found in an examination of the 1998 convective seasons over the central United States that retriggering of deep convection occurred in over half of the MCVs they studied. These MCVs tended to form when weak-to-moderate shear was present, generally weaker shear than in cases of MCSs that did not spawn an observed MCV. The retriggered convection can also reinvigorate the MCV, leading to repeating cycles that can last several days (Rogers and Fritsch 2001; Trier and Davis

2002; Davis and Trier 2002; Conzemius et al. 2007). While many of the studies have focused on MCVs over land, it seems natural to examine the potential influence of an MCV in the formation of a tropical cyclone (e.g., Montgomery et al. 2006).

The present study examines the formation of Hurricane Gabrielle (2001), focusing on whether an initial disturbance and vertical wind shear were favorable for development. These factors are chosen based on theories linking MCVs to tropical cyclone formation (Simpson et al. 1997; Ritchie and Holland 1997; Bister and Emanuel 1997; Montgomery et al. 2006) and linking vertical wind shear to MCV reinvigoration (RJ90). Following these theories, and consistent with the quasigeostrophic omega equation (Sutcliffe 1947; Trenberth 1978), both the vortex and the vertical wind shear are critical to induce vertical motion. Removing or weakening either would reduce the chances of development, or delay development. In their case study of Hurricane Danny (1997), Molinari et al. (2004) found that moderate vertical wind shear acting over the central vortex led to steady intensification, and hypothesized that moderate vertical wind shear accelerated early development. Gabrielle is chosen as an interesting case to study since it formed in the subtropics from a midtropospheric vortex in an area of nonnegligible vertical wind shear.

The examination is performed using the fifth-generation Pennsylvania State University–National Center for Atmospheric Research (NCAR) Mesoscale Model (MM5, version 3.6.0). Three main simulations are run: a control run and two sensitivity experiments. The control run is compared with observations of Gabrielle's formation. The two sensitivity experiments are designed to test the response of the developing tropical cyclone to alterations in the initial conditions. The first sensitivity experiment removes the initial (or precursor) disturbance, a midtropospheric vortex located over Florida. The second sensitivity experiment reduces the vertical wind shear over the area of formation.

The rest of the paper is organized as follows: Section 2 reviews Gabrielle's formation as well as available observations for the days prior to Gabrielle being named a tropical storm. The model configuration and sensitivity experiments are discussed in section 3. In section 4 the results of the simulations are examined and compared to each other and to observations of Gabrielle's formation. A summary of the main findings as well as areas for future research is presented in section 5.

2. Hurricane Gabrielle

The life cycle of Hurricane Gabrielle is summarized in the Tropical Cyclone Report issued by the National Hurricane Center (NHC; http://www.nhc.noaa.gov/2001gabrielle.html). Briefly, the pre-Gabrielle disturbance formed in the Gulf of Mexico near the tail end of a stationary front around 9 September 2001. The disturbance was identified as a tropical depression at 1800 UTC 11 September 2001, and was classified as Tropical Storm Gabrielle at 1200 UTC 13 September 2001. Gabrielle was only 175 n mi southwest of Venice, Florida, when it was declared a tropical storm. It made landfall as a tropical storm near Venice around 1200 UTC 14 September 2001. Gabrielle crossed the Florida peninsula and reemerged into the Atlantic Ocean, where it intensified to hurricane strength by 0000 UTC 17 September 2001. Gabrielle was classified as an extratropical system on 19 September 2001, while off the coast of Newfoundland, Canada. NHC's "best track" for Gabrielle, from 1800 UTC 11 September until 0000 UTC 15 September, is shown in Fig. 1.

Gabrielle's origin was a weak, nearly stationary low- to midlevel trough off the southeastern U.S. coastline on 5 September. The National Centers for Environmental Prediction (NCEP) final operational analysis shows a midtropospheric trough off the southeastern U.S. coastline, extending over northern Florida on 7 September (Fig. 2a). A broad closed circulation centered over Florida can be seen on 8 September (Fig. 2b), with the cutoff low emerging over the Gulf of Mexico by 10 September. A surface low formed in association with the cutoff low on 11 September, resulting in the designation of Tropical Depression 8 at 1800 UTC 11 September, at which point NHC's "best track" data begins. A closed circulation and a positive potential vorticity anomaly can be seen on the 315-K isentrope by 1200 UTC 12 September (Fig. 2f, see arrow). An upper-level trough extends over the region at earlier times (Figs. 2a–d), moving out of the region by 11 September (Fig. 2e). This study focuses on the midlevel precursor to Gabrielle.

The formation of Gabrielle occurred with convection distributed asymmetrically about the center of surface cyclonic circulation. Figure 3a shows scatterometer data on 11 September, and satellite infrared near the time of the Quick Scatterometer (QuikSCAT) pass is shown in Fig. 3b. The convection remained to the south and southwest of the surface center of circulation as indicated by the QuikSCAT pass, and an exposed low-level center can be seen in the visible satellite imagery on 10–11 September (not shown). Although the QuikSCAT winds suggest a frontal structure southeast of the center of circulation, rain contamination and lack of temperature data make it difficult to say a front was present.

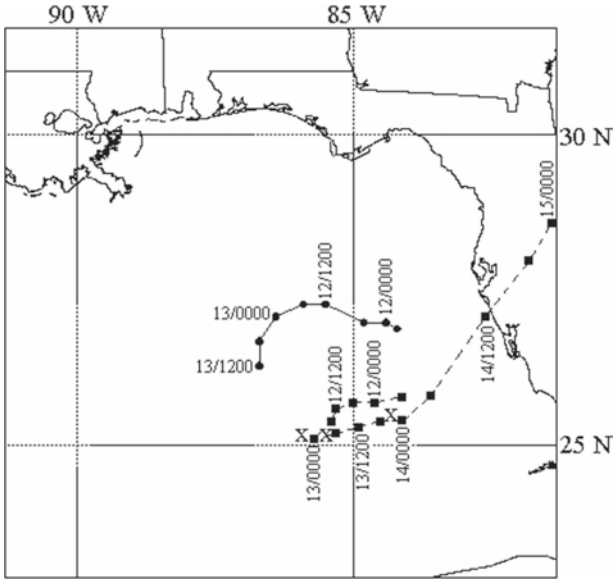

FIG. 1. NHC best-track positions for Hurricane Gabrielle from 1800 UTC 11 Sep to 0000 UTC 15 Sep 2001 (squares, dashed line). Gabrielle was designated a tropical storm at 1200 UTC 13 Sep. Also shown: control run track from 1800 UTC 11 Sep to 1200 UTC 13 Sep (circles, solid line), and NHC advisory positions on 13 Sep (Xs). The leftmost X represents the advisory position on both 0300 and 0900 UTC 13 Sep, the middle X on 1500 UTC 13 Sep, and the rightmost X on 2100 UTC 13 Sep.

Infrared satellite imagery on 11–13 September, overlaid with NHC best-track positions, is shown in Fig. 4. Convection remained generally south and east of the center of circulation as Gabrielle developed. Several distinct mesoscale areas of convection acquired a general southwest-to-northeast orientation on 12 September (Figs. 4d–e). This orientation corresponds approximately to the orientation of midtropospheric cyclonic PV on 12 September (Fig. 2f). The center of circulation drifted southwest until 13 September, when it moved back to the east-northeast and strengthened as the convection organized (Fig. 4f).

While NHC's best track smoothed the movement of the center on 13 September, the forecast advisories contained a more discrete jump in position. The NHC advisories discuss a sudden change in position of Gabrielle's center from 1500 UTC 13 September to 2100 UTC 13 September. The discussion speculates the change could be due to movement of the existing center or to a reformation of the center. Previous to this jump, the broad circulation center moved slowly. The locations for the 13 September forecast advisories are indicated by the Xs in Fig. 1. The system remained nearly stationary from 0300 to 0900 UTC, and shifts slowly eastward by 1500 UTC, before the large shift east by 2100 UTC. This discrepancy, when combined with satellite imagery showing a flare-up and reorganization of convection (Fig. 4f), indicated the possibility that rather than the center moving that distance over a longer time frame, a new center may have formed to the east-northeast of the previous one as Gabrielle organized, causing a jump in position.

Molinari et al. (2006) examined Gabrielle on 14 September using available reconnaissance aircraft, Weather Surveillance Radar-1988 Doppler (WSR-88D), and National Lightning Detection Network (NLDN) data. According to their analysis of the observations, Gabrielle reformed about a new center of circulation downshear of the original center. During this time they found convection to be highly asymmetric with most occurring downshear left of the center of circulation. Similarly, Molinari et al. (2004) found that during the development of Hurricane Danny (1997) the center reformed in downshear convection. Danny went on to axisymmetrize and intensify into a hurricane before landfall, while Gabrielle made landfall as an asymmetric strong tropical storm. The presence of consistent asymmetric convection in Gabrielle during the early stages of development presents the question of whether vertical shear played a favorable role in Gabrielle's formation, which this project examines through simulations.

3. Numerical experiments

a. Model configuration

This study uses the MM5, version 3.6.0 (Grell et al. 1995), for simulating Gabrielle's formation. The configuration of MM5 for the numerical experiments is the same in all simulations, with only the initial conditions varying.

The simulations use three two-way interactive nested grids. The layout of the three domains is shown in Fig. 5. The domains, from outermost to innermost, have grid spacings of 111, 37, and 12.3 km, with 91×91, 79×73, and 91×91 grid points, respectively. All three domains have 38 vertical levels from the surface to 50 hPa, with more closely spaced levels near the surface.

The simulations focus on the early formation of Gabrielle. The simulation period begins over 48 h before the National Hurricane Center started producing advisories for Tropical Depression 8 and ends when the depression was upgraded to a tropical storm and named Gabrielle. Consequently, the simulations cover a 96-h period, from 1200 UTC 9 September 2001 through 1200 UTC 13 September 2001.

Domains 1 and 2 are run for the entire 96-h period from 1200 UTC 9 September to 1200 UTC 13 Septem-

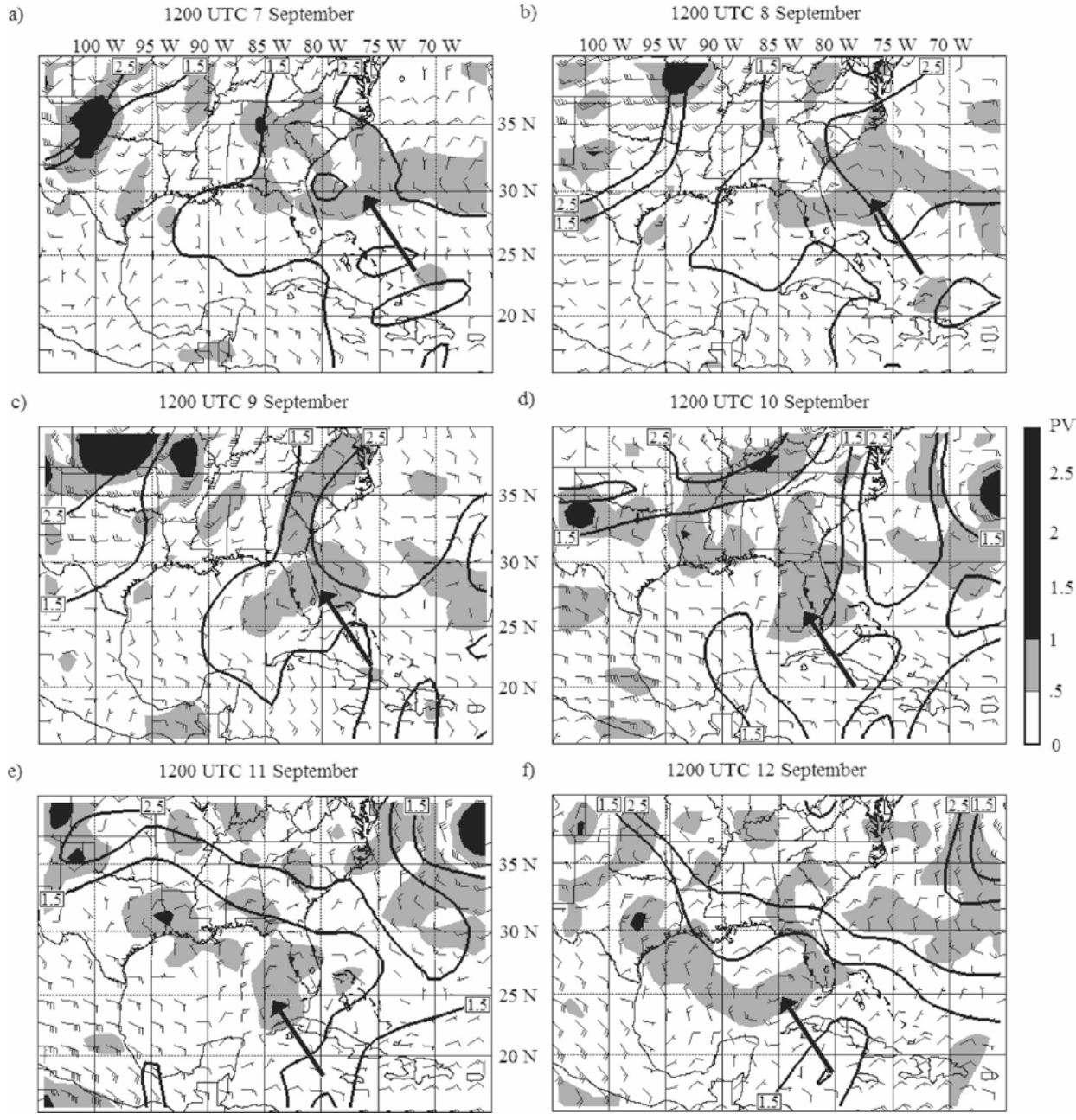

FIG. 2. The NCEP final operational analysis potential vorticity (gray shading) and horizontal winds on the 315-K potential temperature surface for (a) 1200 UTC 7 Sep, (b) 1200 UTC 8 Sep, (c) 1200 UTC 9 Sep, (d) 1200 UTC 10 Sep, (e) 1200 UTC 11 Sep, and (f) 1200 UTC 12 Sep. Also shown are the 1.5- and 2.5-PVU contours on the 350-K potential temperature surface. Arrows point to PV anomaly discussed in text.

ber. Domain 3, the innermost domain, is added to the model 48 h into the simulation, running from 1200 UTC 11 September to 1200 UTC 13 September. Domain 3 is run for only the last 48 h of the simulation to reduce computational requirements.

The time step for the three domains from outermost to innermost is 180, 60, and 20 s, respectively. MM5 produces output every 3 h for domains 1 and 2 and every hour for domain 3.

The physical parameterizations chosen for this study are the numerical weather prediction (NWP) explicit microphysics (NEM) scheme (Schultz 1995), the Kain–Fritsch cumulus scheme (Kain and Fritsch 1993), the Blackadar representation of the planetary boundary

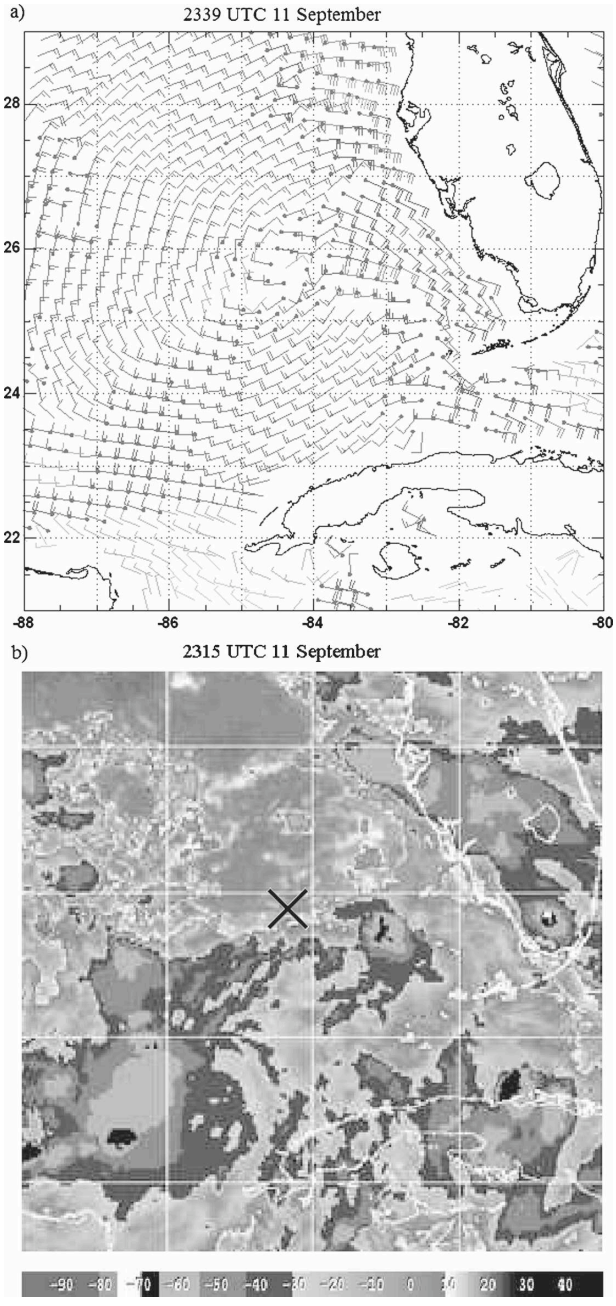

FIG. 3. QuikSCAT-derived surface winds at (a) 2339 UTC 11 Sep and infrared satellite imagery at (b) 2315 UTC 11 Sep. QuikSCAT image from Remote Sensing Systems (www.ssmi.com/qscat/qscat_browse.html) and satellite image from Naval Research Laboratory (NRL) archive (www.nrlmry.navy.mil/tc_pages/tc_home.html). Rain-flagged winds are represented by a circle at the base of the wind vector. The X in (b) represents center of surface circulation as determined from QuikSCAT winds in (a).

layer (PBL; Zhang and Anthes 1982), cloud radiation, a multilayer soil temperature model, and no shallow convection. The NEM scheme is chosen as an efficient scheme that includes rain, snow, and graupel, while the Kain–Fritsch cumulus scheme is chosen as a sophisticated representation of clouds. The Blackadar PBL scheme is chosen for its simplicity compared to other schemes and for having a higher reliability in strong surface winds than the medium-range forecast model PBL scheme (MRF; Hong and Pan 1996; Braun and Tao 2000). The Kain–Fritsch scheme is used in all three domains, as domain 3's 12.3-km grid spacing is too large to rely on explicit convection. Given the importance of convection in the processes being examined, future work includes reducing the grid spacing of the innermost domain to allow for explicit convection.

The simulations use the NCEP final operational analysis to initialize MM5. The NCEP analysis data provides both the initial conditions and the boundary conditions. The boundary conditions are updated by tendency every 6 h. The control run uses the unaltered analysis for its initial conditions, while each of the two sensitivity experiments alters the initial conditions from the analysis as described below.

b. Removed initial disturbance (RID) experiment

In the first sensitivity experiment the initial disturbance is removed. Based on the large-scale environment in which Gabrielle formed and studies examining tropical cyclogenesis from MCVs and MCV-type precursors (Bister and Emanuel 1997; Simpson et al. 1997; Ritchie and Holland 1997; Montgomery et al. 2006), the initial disturbance is chosen to be the midtropospheric vortex located over Florida on 9 September (Fig. 3c).

To accomplish this, the PV anomaly attributed to the midtropospheric vortex is removed following the methodology described in Davis and Bosart (2002). The technique for removing the PV anomaly is summarized as follows and is shown in Fig. 6: A box is placed in low-PV areas surrounding the positive PV anomaly, covering an area spanning a few hundred kilometers in each horizontal direction. The PV within the box is averaged along zonal lines of grid points (Fig. 6a). The center value along each zonal line is replaced by the average PV for that line, and the PV field is altered to vary linearly between the average at the center and the original value at each endpoint of the zonal line (Fig. 6b). This box extends vertically from 900 to 300 hPa to capture the entirety of the PV anomaly without involving upper-level events. The modified PV field has the same volume-integrated PV as the original PV field.

The new PV field is inverted to compute balanced wind and temperature increments associated with the PV modifications. Nonlinear balance is assumed, as used in Davis and Bosart (2002). The balanced increments are added to the model initial conditions (inter-

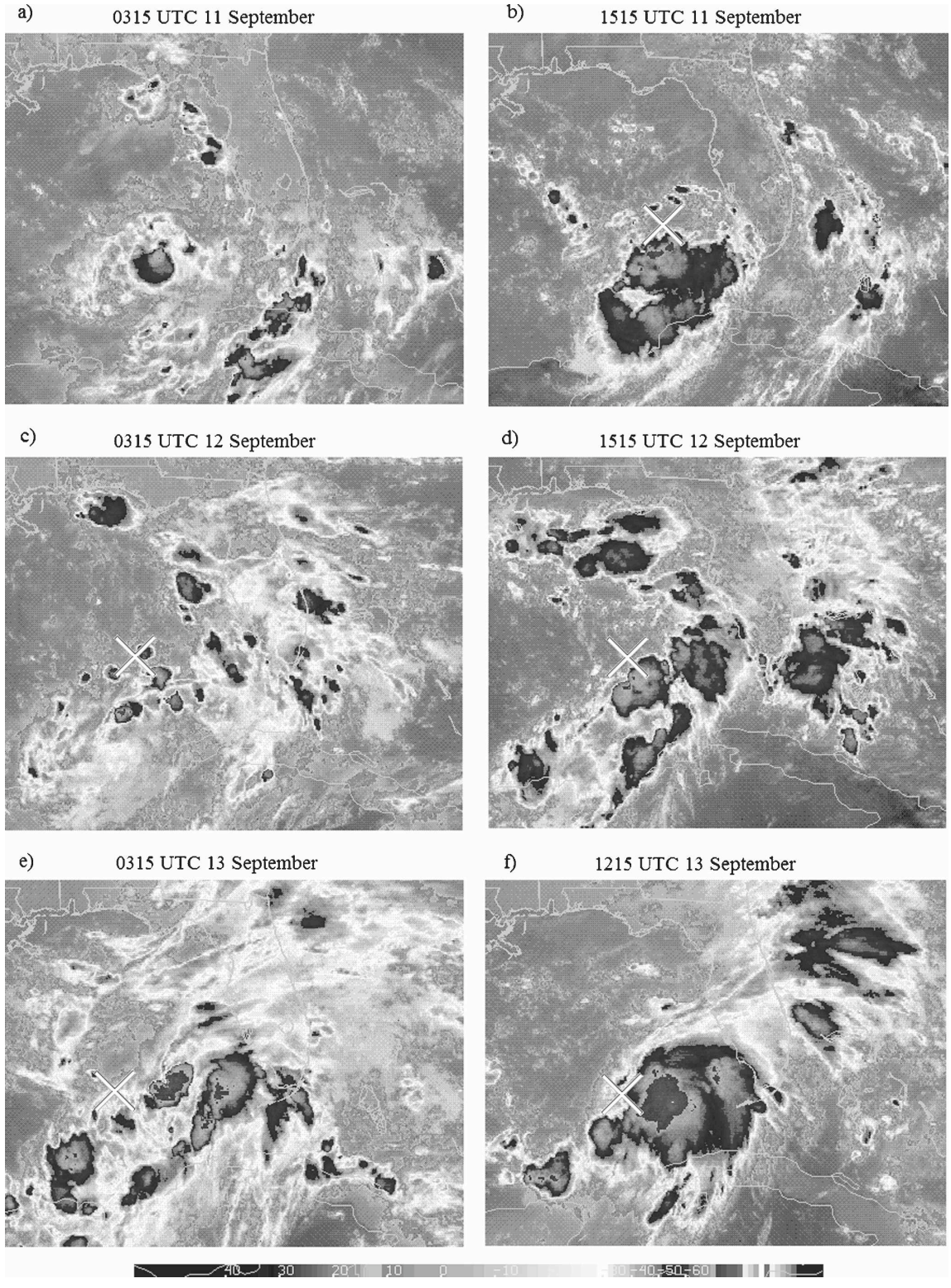

FIG. 4. Infrared satellite images [provided by the Cooperative Institute for Research in the Atmosphere (CIRA)] for (a) 0315 UTC 11 Sep, (b) 1515 UTC 11 Sep, (c) 0315 UTC 12 Sep, (d) 1515 UTC 12 Sep, (e) 0315 UTC 13 Sep, and (f) 1215 UTC 13 Sep. The X designates NHC best-track position [not available in (a)].

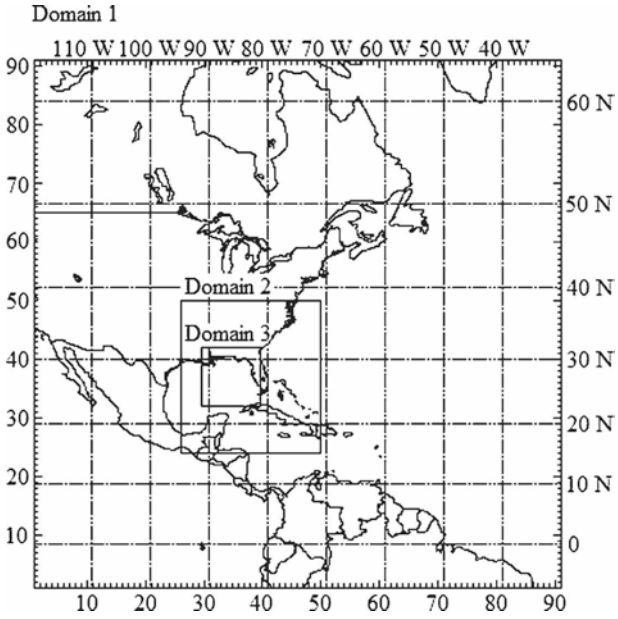

FIG. 5. The three domains used in the MM5 simulations. Grid points on the outermost domain are indicated by the left and bottom axes; latitude and longitude on the right and top axes, respectively.

polated vertically to the model levels) and the RID simulation is run. Figure 7a shows the initial PV and wind vectors at 600 hPa in the area surrounding the initial disturbance in the control run, while Fig. 7b shows those fields in the initial conditions for RID. After the procedure, the positive PV anomaly has disappeared, while still leaving the flow several hundred kilometers distant relatively unchanged.

c. *Reduced vertical wind shear (RVS) experiment*

In the second sensitivity experiment the vertical wind shear profile is altered over a large area around the initial disturbance. The alterations are based on the fact that horizontal gradients in PV are inversely related to velocity through the invertibility principle (Hoskins et al. 1985). Thus removal of PV gradients over a deep layer will tend to weaken the velocity at all layers and hence decrease the shear. In practice, local alterations of PV are effective for decreasing the shear within a subsynoptic-scale region, while retaining a significant barotropic component of the flow associated with PV features on larger scales. The retained barotropic component allows the path of the remaining disturbance to be relatively unchanged from the path of the disturbance in the control simulation. This approach assumes that the shear is due to the balanced part of the flow.

In the present case, the alterations are performed by removing the horizontal gradient of PV along pressure levels, from 900 to 300 hPa. The stepwise process first uses the method described for RID to remove the PV anomaly attributed to the initial disturbance. Next, PV is averaged over a larger-scale box, roughly 1100 km on a side (11×10 grid points on domain 1). This domain is chosen so that the PV on the boundaries is approximately uniform. To reduce the remaining vertical wind shear, a positive PV anomaly is added in the upper atmosphere and a negative temperature anomaly is added to the lower atmosphere over the western Gulf of Mexico. Finally, the PV anomaly of the initial disturbance is added back to the modified PV. This new PV field is inverted to compute balanced wind and temperature increments associated with the PV modifications. These are added to the model initial conditions (interpolated vertically to model levels) and the RVS simulation is run. The removal and reinsertion of the PV anomaly associated with the initial disturbance is performed to alter the vertical wind shear without also removing the initial disturbance examined in RID.

Figures 8a and 8b show the initial 600-hPa PV and the 0–6-km vertical wind shear vectors for the control run and for RVS, respectively. While the shear has not

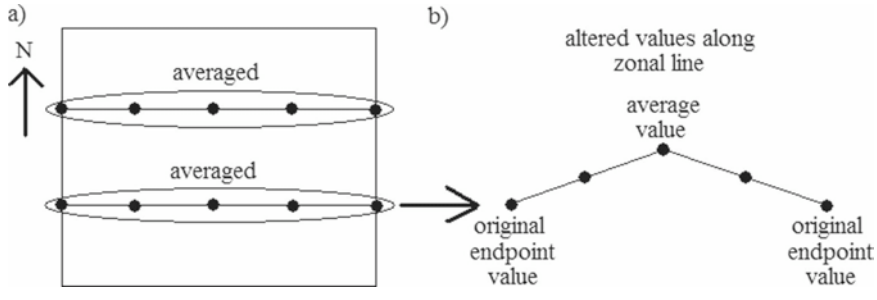

FIG. 6. (a) Horizontal cross section of PV alteration technique. (b) Sample zonal line showing alterations to values of PV. Grid points along each zonal line are averaged; then the average value is assigned to the center grid point and the rest of the grid points are altered to vary linearly between the original endpoints and the central average value.

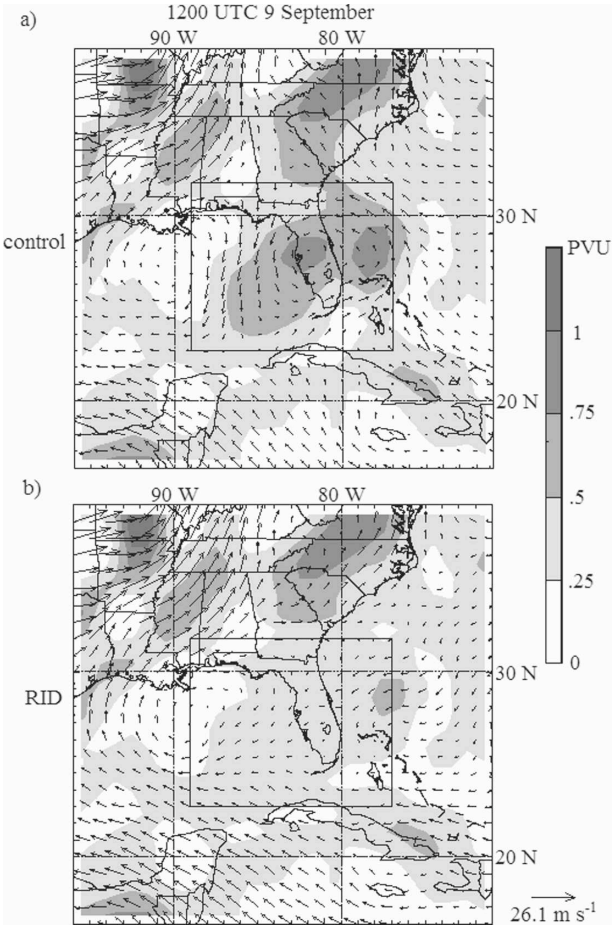

FIG. 7. The potential vorticity (contours every 0.25 PVU) and horizontal wind vectors (maximum vector indicated) at 600 hPa for (a) the control run and (b) after altering the potential vorticity field for RID. Box indicates region of PV averaging.

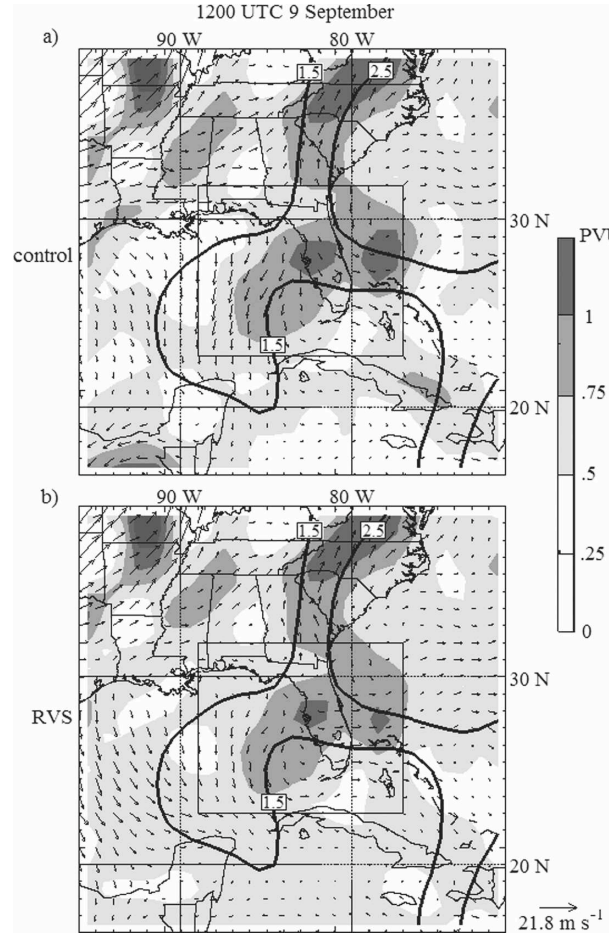

FIG. 8. The potential vorticity (contours every 0.25 PVU) at 600 hPa and local 0–6-km shear vectors (maximum vector indicated) for (a) the control run and (b) after altering the vertical wind shear for RVS. Box indicates area of PV anomaly removal and then reinsertion. Also shown are the 1.5- and 2.5-PVU contours on the 350-K potential temperature surface.

been entirely removed from RVS's initial conditions, it has been lessened significantly with minimal alteration of the initial disturbance. The black contours in Fig. 8 highlight the focus in RVS of altering the vertical wind shear over the midtropospheric initial disturbance—without changing the upper-level structure to maintain consistency with RID. The altered shear values over the western portion of the Gulf of Mexico in Fig. 8b are due to the additional measures taken to further reduce the shear over the area of the disturbance.

4. Results

The control run is compared with observations of intensity, track, and convection during Gabrielle's formation, and the simulation is examined to gain a better understanding of the convective processes being represented in the model. The sensitivity experiments are then discussed, and RVS is further investigated.

a. Control run

Both minimum central pressure and maximum sustained winds are used as measures of intensity. NHC's best track for Gabrielle begins at 1800 UTC 11 September, 54 h into the control run. The control run's minimum central pressure is equal to or less than the NHC best track for the entirety of the simulation, differing by at most 3 hPa (Fig. 9). Both show an almost steady decrease in pressure, an indication of an intensifying system.

The control run also shows maximum surface winds similar to the NHC best track's maximum sustained winds (Fig. 10). Both the model and the best-track winds are valid 10 m above the surface. The control run and the best track differ by less than 5 m s^{-1} at any point between 1800 UTC 11 September (54 h) and 1200

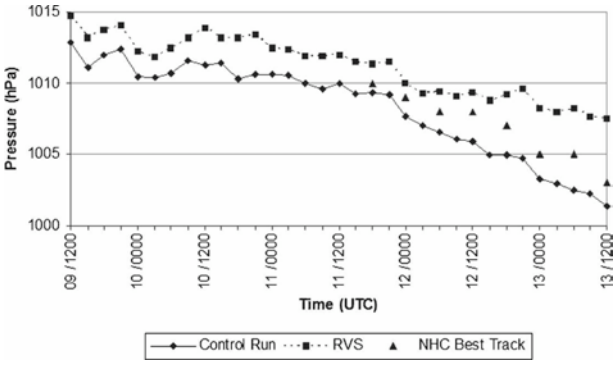

FIG. 9. Minimum central pressure (hPa) of the pre-Gabrielle disturbance for both the control run (solid line, diamonds) and RVS (dashed line, squares). NHC best-track minimum central pressure (triangles) also shown when available (every 6 h starting 1800 UTC 11 Sep).

UTC 13 September (96 h), with the largest differences occurring at the beginning of the best track and at the end of the simulation, with the control run having lower maximum surface winds in both cases. The control run and the NHC best track both indicate maximum surface winds holding steady from 1800 UTC 11 September until 0000 UTC 12 September. At this point, the model maximum surface winds increase for approximately 18 h. The NHC best track also increased maximum sustained winds, but at a slower pace. This leads to good agreement between the control run and the best track, from 0600 UTC 12 September to 0600 UTC 13 September. Reconnaissance aircraft first flew into Gabrielle at approximately 0000 UTC 13 September, providing additional information on which to base the best track. Another detail to consider in the comparison is that NHC reports maximum sustained winds in increments of 5 kt, or approximately 2.5 m s^{-1}.

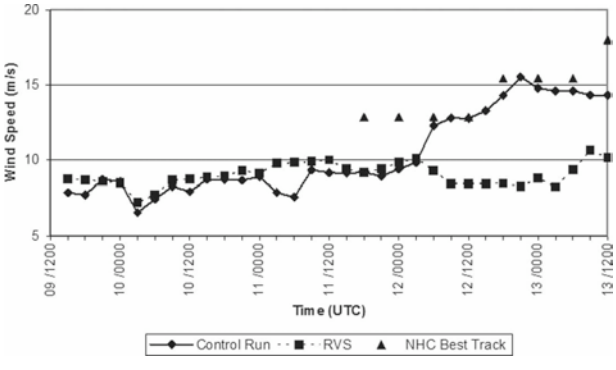

FIG. 10. Maximum surface wind speed (m s^{-1}) of the pre-Gabrielle disturbance for the control run (solid line, diamonds) and RVS (dashed line, squares). NHC best-track maximum sustained winds (triangles) also shown when available (every 6 h starting 1800 UTC 11 Sep).

The control run consistently places the developing storm north of the NHC best track by 1°–2° for the entirety of the simulation (Fig. 1). Part of the difference between the best track and the control run is likely caused by the difference in the initial positions, which could be due to the resolution of the NCEP analysis and the broadness of the circulation. Regardless, both tracks keep the system over water for the duration of the simulation, with little difference in model sea surface temperatures between the best track and the simulated track. The model track deviates about 2° west of the NHC best track toward the end of the control run, after 0000 UTC 13 September (84 h into simulation). The comparison of the best track to the forecast advisories for Gabrielle in section 2 (Fig. 1) indicates that the change in movement of the center of circulation to the northeast may be a more abrupt change than is seen in the smoothed best track, and takes place after the period covered by the simulation. This change in motion occurred after a flare-up of convection to the northeast; a new center may have emerged from the vorticity maximum developing in association with that convection.

To examine the mesoscale convective features of the control run, the cloud-top temperature field is compared with available IR satellite imagery. Figure 11 shows the model cloud-top temperatures produced by domain 2 (cropped for easier comparison with Fig. 4) at six different times in the control run. This comparison provides a general measure of the strength and location of convection associated with Gabrielle.

Throughout the simulation period the control run shows more widespread cold cloud tops than the satellite images. This is to be expected since the coarseness of the grid necessitates a parameterization for convection instead of explicit convection and the grid aspect of the model does not allow for shallow layers of clouds that appear partly transparent, unlike satellite imagery. Although the model has more widespread cold cloud tops, the trends seen in the simulation are similar to the observed satellite images.

Both the satellite infrared images and the simulation output indicate general agreement in the location of convection relative to the disturbance. The control run places deep convection downshear of the center of the disturbance throughout the simulation period, and shows the convection organizing around the disturbance by the end of the simulation period. The qualitative similarities between the observations and the control run encourage further examination of the simulated convection for additional information on Gabrielle's development.

Examining the progression of the low-level vorticity

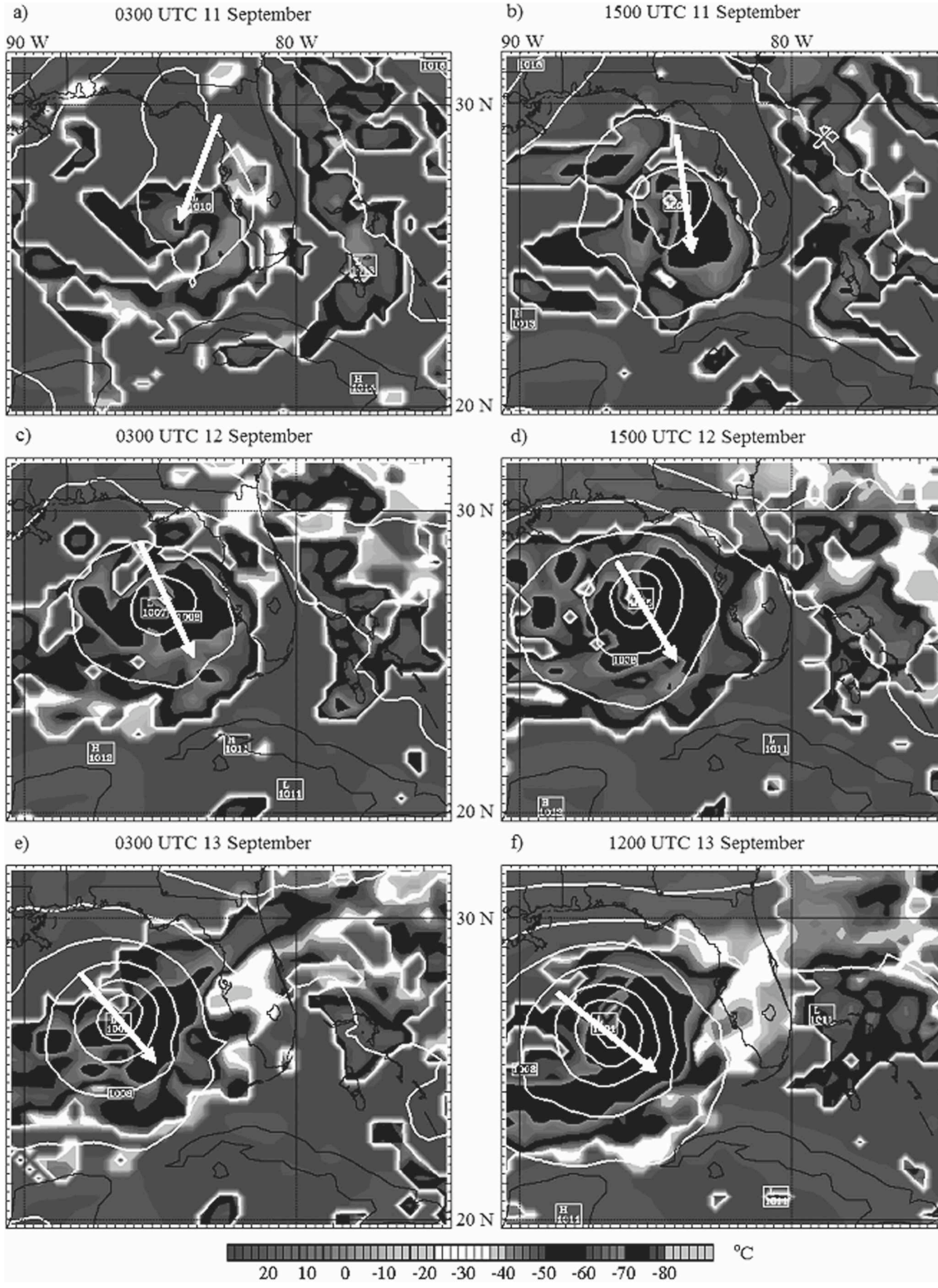

FIG. 11. Control run cloud-top temperatures (gray shading) and sea level pressure (white contours every 2 hPa) on domain 2 for (a) 0300 UTC 11 Sep, (b) 1500 UTC 11 Sep, (c) 0300 UTC 12 Sep, (d) 1500 UTC 12 Sep, (e) 0300 UTC 13 Sep, and (f) 1200 UTC 13 Sep. White arrows indicate the direction of the vertical wind shear over the system.

associated with the system shows a wide area of positive vorticity at 1500 UTC 11 September (Fig. 12a) developing into an organized ring of high vorticity by 1200 UTC 13 September (Fig. 12b). Taking a cross section of vorticity along the vertical shear vector, centered on the center of circulation of the pre-Gabrielle disturbance (Fig. 12a) at 1500 UTC 11 September provides further information about the vorticity structure. In the control run (Fig. 13a) the vorticity noticeably tilts downshear with height, to the point where the center of circulation of the system is downshear of the low-level center of circulation. On 11 September, visible satellite imagery reveals an exposed low-level center of circulation in Gabrielle (not shown). At low levels there is a positive vorticity anomaly downshear of the center of circulation. The positive vorticity anomaly downshear of the center of circulation remains a consistent feature throughout most of the control run.

b. *RID experiment*

A significant difference is observed in the model output after removing the initial disturbance. Despite deep convective activity in the Gulf of Mexico comparable in amount to the other simulations in terms of cloud-top temperatures, rainfall patterns reveal no organization into a tropical system (not shown). The low-level vorticity (Figs. 12c,d) does not show any evolution toward a state consistent with a developing tropical cyclone. No evidence of a pre-Gabrielle disturbance is found during the four days of simulation. The lack of development in RID, when combined with the choice to limit alterations to the low- to midlevels while leaving the upper-level structure intact, suggests that the upper-level trough in Fig. 2 had little direct impact on Gabrielle's formation.

c. *RVS experiment*

In examining RVS, the first question is whether the vertical wind shear was reduced over the pre-Gabrielle disturbance. Figure 8b shows that to be the case in the initial conditions. Figure 14 shows the time series of vertical wind shear for both the control run and RVS. The vertical wind shear is calculated over the 900–500-hPa layer in a 300 km $\times$ 300 km box over the developing system. The vertical wind shear typically used to determine significant values for hindering formation or intensification is over a deeper layer than the vertical wind shear calculated here.

The vertical wind shear over the developing system is reduced not only during the initial time period, but throughout the entirety of RVS. For most of RVS the vertical wind shear reduces its magnitude by half compared to the control run. The vertical wind shear in RVS maximizes at about 5 m s^{-1}, as compared with just over 10 m s^{-1} in the control run. That maximum is seen at the same time in both simulations, at 1200 UTC 12 September (72 h into simulation; Fig. 14).

Examining the same measures of intensity used for the control run, RVS produces a much weaker version of Gabrielle by the end of the simulation period. The minimum central sea level pressure shown in Fig. 9 indicates that RVS deepens Gabrielle less than one-half of the amount of the control run, or even the best track over the same time period. The difference between the simulations is also seen in the maximum surface winds (Fig. 10), where RVS intensifies less than the control run and best track. Both measures indicate a weaker final system in RVS than either the control run or best track. While some differences exist between the control run and RVS throughout the time period, the two simulations show a distinct divergence in both intensity measures after 0300 UTC 12 September (63 h into the simulation).

Comparison between the control run and RVS attempts to identify how this divergence came about. The structure of the pre-Gabrielle disturbance in RVS is very different from the control run. In Fig. 12, the low-level horizontal vorticity is more linear in RVS than in the control run at 1500 UTC 11 September and is not oriented along the vertical shear vector (as can be seen by the cross-section orientation). The elongated structure in RVS has wrapped up into a more circular feature by 1200 UTC 13 September, but is weaker than in the control run, with areas of negative relative vorticity still located relatively close to the system. Examining the vertical cross sections in Fig. 13 for 1500 UTC 11 September indicates differences in the vertical structure as well. The system in RVS is less tilted than the control run and has higher values of relative vorticity in the boundary layer. The control run, however, has higher values of relative vorticity extending farther up in the troposphere, and a broader region of positive relative vorticity about the center of circulation. As discussed previously, the control run has positive relative vorticity consistently located downshear of the center of circulation, in accordance with the focusing of convection downshear of the vortex. This tendency is not seen in RVS; rather convection is collocated with the center of circulation.

Given the difference in structure and intensity between the systems in the control run and RVS, an interesting question is when these systems transitioned into warm-core tropical systems. This is assessed using the potential temperature difference between the center of circulation and the environment (175 km radius

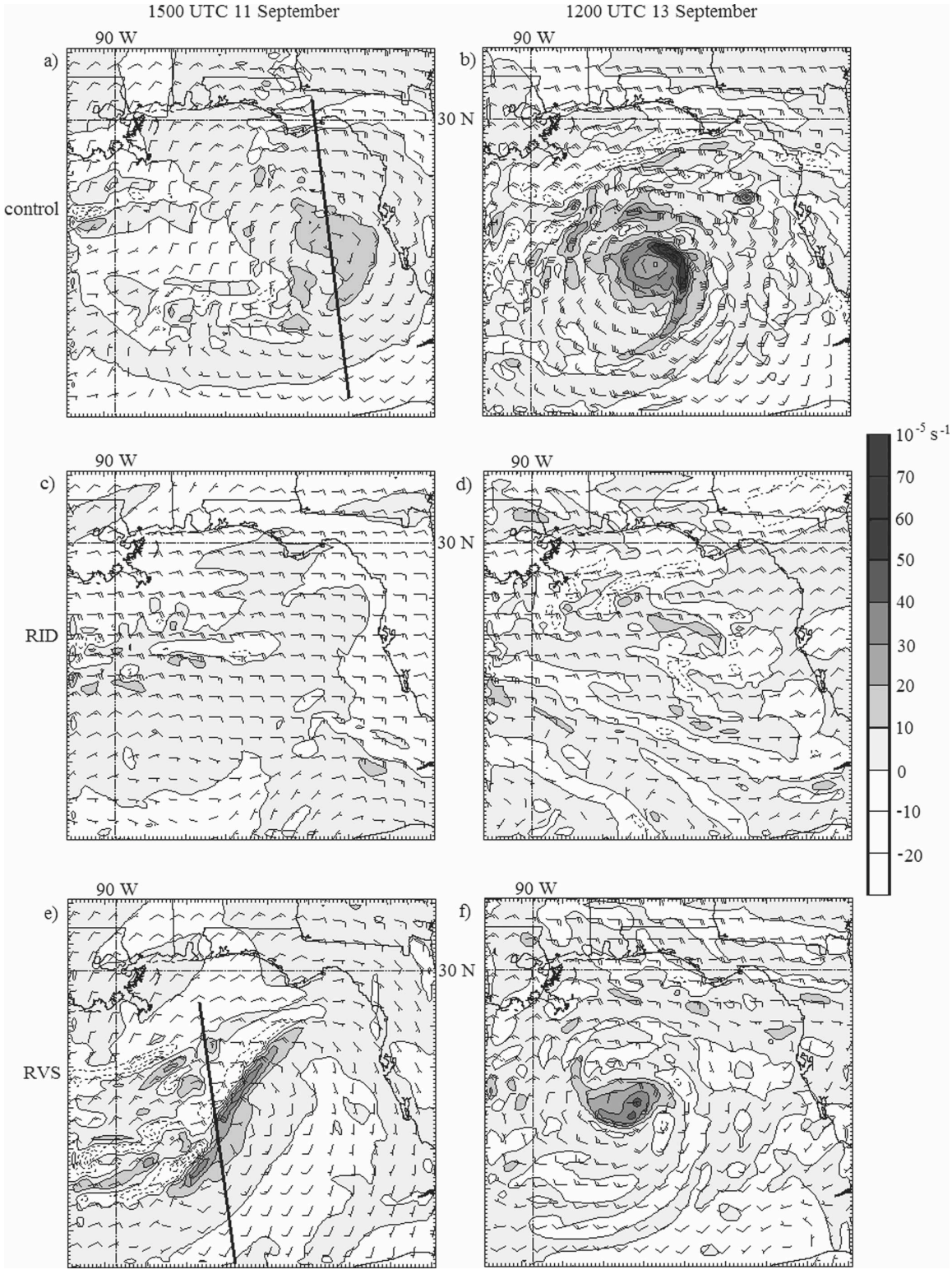

FIG. 12. Relative vorticity (gray shading for positive values, dashed contours for negative values) and horizontal winds at 900 hPa on domain 3 for 1500 UTC 11 Sep (51 h) and 1200 UTC 13 Sep (96 h), respectively, for (a), (b) the control run, (c), (d) RID, and (e), (f) RVS. Black line in (a) and (e) represents where the vertical cross section is taken for Figs. 13a and 13b, respectively.

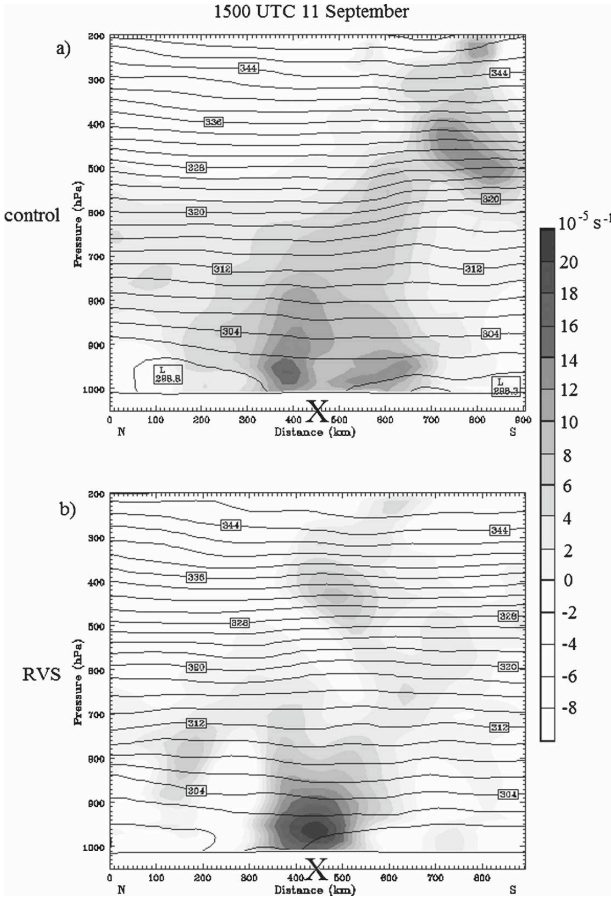

FIG. 13. Vertical cross section of vorticity (gray shading) and potential temperature (black contours every 2 K) on domain 2 for (a) control run and (b) RVS at 1500 UTC 11 Sep. Cross section was taken along the vertical shear vector, centered on the center of circulation of the pre-Gabrielle system (designated by X on horizontal axis), as shown in Fig. 12a for control run and Fig. 12e for RVS.

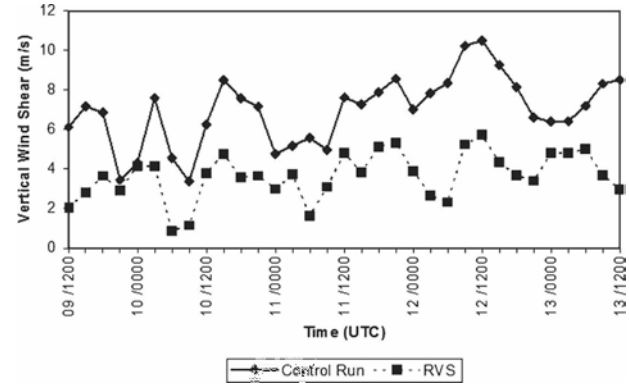

FIG. 14. Magnitude of vertical wind shear (m s^{-1}) over the pre-Gabrielle disturbance for the control run (solid line, diamonds) and RVS (dashed line, squares). Vertical shear is calculated over the 900–500-hPa layer, in a 300 km by 300 km box centered on the system.

from the center), averaged over the 900–600-hPa layer (Fig. 15). The control run has a sustained low-level warm core starting at about 1200 UTC 10 September (24 h into the simulation). RVS does not show a sustained warm core until over 60 h into the simulation, at 0300 UTC 12 September (63 h). This indicates that the differences between the control run and RVS at earlier times may be important in the eventual intensification of the control run relative to RVS.

To further examine the difference between the control run and RVS at early times, a measure of the integrated vorticity of each system is calculated over a 220 km × 220 km box centered on the center of circulation, over the 900–500-hPa layer (Fig. 16). The integrated vorticity of the initial disturbance in RVS is slightly weaker than the control run, but the difference is small and actually reduces over the first 9 h of the simulations. However, at 12 h (0000 UTC 10 September) the two simulations diverge. The integrated vorticity in RVS decreases, while the decrease is not seen in the control run. This difference is reflected at later times in the smaller region of positive vorticity in RVS compared to the control run (Figs. 13, 14), despite a higher maximum of vorticity in RVS (Fig. 14). The decrease in the integrated vorticity of the system in RVS is consistent with a decrease in the precipitation over the previous 6 h relative to the control run (Fig. 17).

In summary the reduction of the vertical wind shear led to a weaker version of Gabrielle than was seen in the control run or observations of the actual case. We contend that this is caused by a lack in RVS of the vertical wind shear serving to focus convection downshear of the original midtropospheric vortex. The dif-

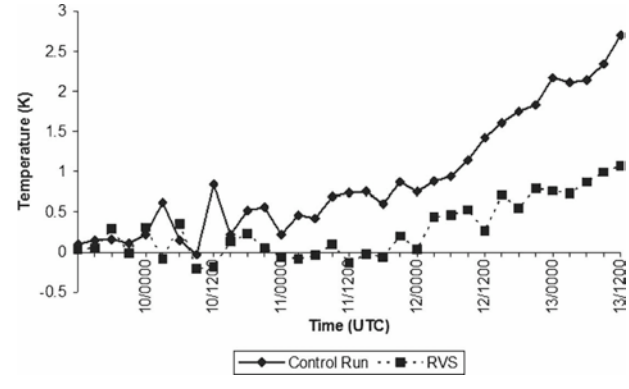

FIG. 15. Time series of the difference between the potential temperature (K) at the center of the system and the potential temperature in the environment (175 km radius from the center), averaged over the 900–600-hPa layer, for both the control run (solid line, diamonds) and RVS (dashed line, squares).

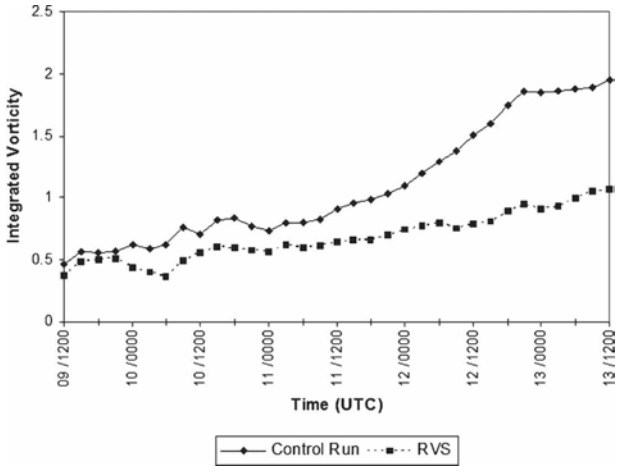

FIG. 16. Time series of the integrated vorticity about Gabrielle's center of circulation for both the control run (solid line, diamonds) and RVS (dashed line, squares). The integrated vorticity is calculated over a 220 km × 220 km box centered on the center of circulation, over the 900–500-hPa layer.

ference in structure led to the slower development of a warm core and subsequent intensification.

5. Conclusions

This study simulates the formation of Hurricane Gabrielle (2001), focusing on whether an initial disturbance and vertical wind shear were favorable for development. Numerical experiments are performed using MM5. The control run examines Gabrielle's formation without any changes to the initial conditions. The first sensitivity experiment, RID, removes the initial disturbance—a midtropospheric vortex. The second sensitivity experiment, RVS, reduces the vertical shear over the area of formation.

The control run reasonably reproduces the major features in the formation of Gabrielle, including intensity estimates and mesoscale convective features. The removal of the initial positive PV anomaly in RID produces a dramatic change in the simulation results. No tropical cyclone formation occurs during the 96-h run. This is to be expected based on studies of the importance of the precursor disturbance in tropical cyclone formation (Gray 1968). The lack of development after removing the midtropospheric vortex supports the hypothesis that MCVs can initiate tropical cyclogenesis (e.g., Simpson et al. 1997; Ritchie and Holland 1997; Bister and Emanuel 1997; Montgomery et al. 2006).

The reduction of the vertical wind shear in RVS creates some interesting differences from the control run. While RVS still produces a system that could be identified as Gabrielle, the system is significantly weaker

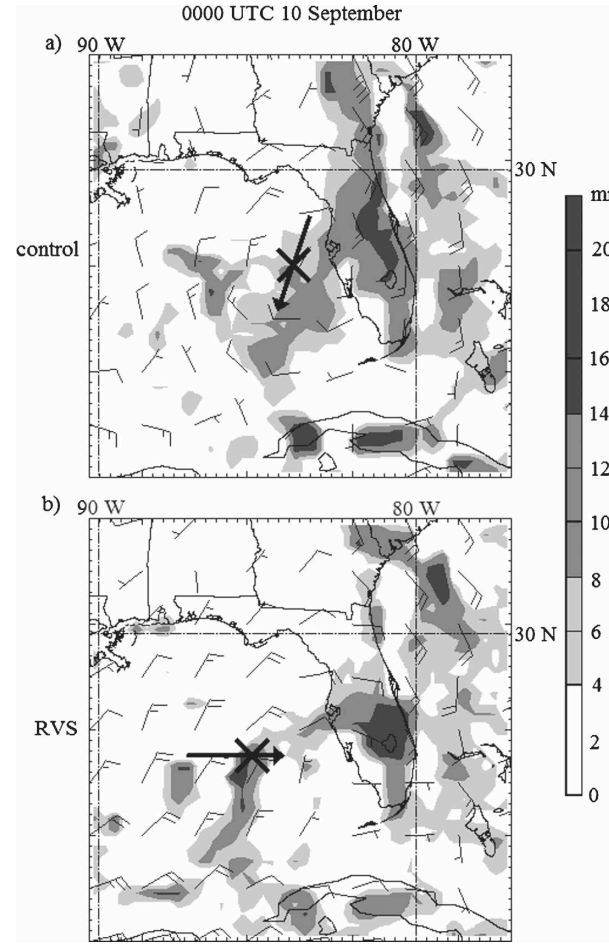

FIG. 17. Six-hour precipitation totals and horizontal winds at 900 hPa at 0000 UTC 10 Sep (12 h) for (a) the control run and (b) RVS. The Xs indicate center of circulation at time shown, and arrows indicate direction of vertical wind shear over the center of circulation averaged over the 6-h period of precipitation accumulation (1800 UTC 9–0000 UTC 10 Sep).

than either the control run or observations of the actual case.

It is important to examine why the reduction in vertical wind shear led to a weaker version of Gabrielle. In accordance with the theories presented in RJ90 and Raymond (1992), the vertical wind shear acting on a positive PV anomaly will result in mesoscale ascent focused downshear of the anomaly. This ascent will focus convection downshear of the vortex, and the convectively generated PV anomalies can then be axisymmetrized, strengthening the original vortex. The convectively generated anomalies can even be strong enough to become the new center of circulation, axisymmetrizing the old center—this option generally applies when the original vortex is still weak, so is more applicable to tropical cyclogenesis than mature tropical cyclones (e.g., Molinari et al. 2004).

In the control run convection is consistently generated downshear of the center of circulation, in agreement with these theoretical processes. In contrast to the control run, in RVS the development does not show a preferred region of convection in relation to the center of circulation. This system seems to take longer to organize, transitioning to a warm-core system much later than the control run. Molinari et al. (2004) hypothesize that moderate vertical wind shear may act to accelerate tropical cyclogenesis, and it appears in this study to be the case for the formation of Gabrielle.

Whether the results found here with Gabrielle are the consequence of the particular case chosen or can be seen in other cases of tropical cyclogenesis is an area for future study. Davis and Bosart (2002) note the sensitivity of simulations of tropical cyclogenesis to factors including the choice of cumulus parameterization, so further examination of the choice of cumulus parameterization and comparison with explicit convection would be beneficial. Decreasing the grid spacing to allow for explicit convection would also allow for a more thorough investigation of the processes involved in formation in both the control run and RVS.

Further investigation of the effects of vertical wind shear could lead to a better understanding of a possible optimal value or range of values for vertical wind shear for tropical cyclone formation. This in turn could improve forecasts of tropical cyclogenesis. Additional potentially important factors in determining an optimal vertical wind shear include the vertical structure of the shear, the layer over which the shear is considered, and whether current observations contain sufficient detail to resolve the vertical wind shear.

Acknowledgments. The authors thank R. Zehr and S. Murillo for their assistance in procuring observations used in this study. This work was done under the auspices of the Significant Opportunities in Atmospheric Research and Science program of the University Corporation for Atmospheric Research, with funding from the National Science Foundation, the U.S. Department of Energy, the National Oceanic and Atmospheric Administration, the Cooperative Institute for Research in Environmental Sciences, and the National Aeronautics and Space Administration. This material is based upon work supported under a National Science Foundation Graduate Research Fellowship.

REFERENCES

Bister, M., and K. A. Emanuel, 1997: The genesis of Hurricane Guillermo: TEXMEX analyses and a modeling study. *Mon. Wea. Rev.,* **125,** 2662–2682.

Bosart, L. F., and J. A. Bartlo, 1991: Tropical storm formation in a baroclinic environment. *Mon. Wea. Rev.,* **119,** 1979–2013.

Bracken, W. E., and L. F. Bosart, 2000: The role of synoptic-scale flow during tropical cyclogenesis over the North Atlantic Ocean. *Mon. Wea. Rev.,* **128,** 353–376.

Braun, S. A., and W.-K. Tao, 2000: Sensitivity of high-resolution simulations of Hurricane Bob (1991) to planetary boundary layer parameterizations. *Mon. Wea. Rev.,* **128,** 3941–3961.

Conzemius, R. J., R. W. Moore, M. T. Montgomery, and C. A. Davis, 2007: Mesoscale convective vortex formation in a weakly sheared moist neutral environment. *J. Atmos. Sci.,* **64,** 1443–1466.

Davis, C. A., and L. F. Bosart, 2001: Numerical simulations of the genesis of Hurricane Diana (1984). Part I: Control simulation. *Mon. Wea. Rev.,* **129,** 1859–1881.

——, and ——, 2002: Numerical simulations of the genesis of Hurricane Diana (1984). Part II: Sensitivity of track and intensity prediction. *Mon. Wea. Rev.,* **130,** 1100–1124.

——, and S. B. Trier, 2002: Cloud-resolving simulations of mesoscale vortex intensification and its effect on a serial mesoscale convective system. *Mon. Wea. Rev.,* **130,** 2839–2858.

——, and L. F. Bosart, 2003: Baroclinically induced tropical cyclogenesis. *Mon. Wea. Rev.,* **131,** 2730–2747.

DeMaria, M., J. A. Knaff, and B. H. Connell, 2001: A tropical cyclone genesis parameter for the tropical Atlantic. *Wea. Forecasting,* **16,** 219–233.

Gray, W. M., 1968: Global view of the origin of tropical disturbances and storms. *Mon. Wea. Rev.,* **96,** 669–700.

Grell, G. A., J. Dudhia, and D. R. Stauffer, 1995: A description of the fifth-generation Penn State/NCAR Mesoscale Model (MM5). NCAR Tech. Note NCAR/TN-398+STR, 121 pp.

Haynes, P. H., and M. E. McIntyre, 1987: On the evolution of vorticity and potential vorticity in the presence of diabatic heating and frictional or other forces. *J. Atmos. Sci.,* **44,** 828–841.

Hong, S.-Y., and H.-L. Pan, 1996: Nonlocal boundary layer vertical diffusion in a medium-range forecast model. *Mon. Wea. Rev.,* **124,** 2322–2339.

Hoskins, B. J., M. E. McIntyre, and A. W. Robertson, 1985: On the use and significance of isentropic potential vorticity maps. *Quart. J. Roy. Meteor. Soc.,* **111,** 877–946.

Kain, J. S., and J. M. Fritsch, 1993: Convective parameterization for mesoscale models: The Kain–Fritsch scheme. *The Representation of Cumulus Convection in Numerical Models, Meteor. Monogr.,* No. 46, Amer. Meteor. Soc., 165–170.

McBride, J. L., and R. Zehr, 1981: Observational analysis of tropical cyclone formation. Part II: Comparison of non-developing versus developing systems. *J. Atmos. Sci.,* **38,** 1132–1151.

Molinari, J., D. Vollaro, and K. L. Corbosiero, 2004: Tropical cyclone formation in a sheared environment: A case study. *J. Atmos. Sci.,* **61,** 2493–2509.

——, ——, ——, P. Dodge, and F. Marks Jr., 2006: Mesoscale aspects of the downshear reformation of a tropical cyclone. *J. Atmos. Sci.,* **63,** 341–354.

Möller, J. D., and M. T. Montgomery, 2000: Tropical cyclone evolution via potential vorticity anomalies in a three-dimensional balance model. *J. Atmos. Sci.,* **57,** 3366–3387.

Montgomery, M. T., and R. J. Kallenbach, 1997: A theory for vortex Rossby-waves and its application to spiral bands and intensity changes in hurricanes. *Quart. J. Roy. Meteor. Soc.,* **123,** 435–465.

——, and J. Enagonio, 1998: Tropical cyclogenesis via convectively forced vortex Rossby waves in a three-dimensional quasigeostrophic model. *J. Atmos. Sci.,* **55,** 3176–3207.

——, M. E. Nicholls, T. A. Cram, and A. B. Saunders, 2006: A

vortical hot tower route to tropical cyclogenesis. *J. Atmos. Sci.,* **63,** 355–386.

Palmen, E., 1948: On the formation and structure of tropical cyclones. *Geophysica,* **3,** 26–38.

Raymond, D. J., 1992: Nonlinear balance and potential-vorticity thinking at large Rossby number. *Quart. J. Roy. Meteor. Soc.,* **118,** 987–1015.

——, and H. Jiang, 1990: A theory for long-lived mesoscale convective systems. *J. Atmos. Sci.,* **47,** 3067–3077.

Reed, R. J., D. C. Norquist, and E. E. Recker, 1977: The structure and properties of African wave disturbances as observed during phase III of GATE. *Mon. Wea. Rev.,* **105,** 317–333.

Riehl, H., 1948: On the formation of typhoons. *J. Meteor.,* **5,** 247–264.

Ritchie, E. A., and G. J. Holland, 1997: Scale interactions during the formation of Typhoon Irving. *Mon. Wea. Rev.,* **125,** 1377–1396.

Rogers, R. F., and J. M. Fritsch, 2001: Surface cyclogenesis from convectively driven amplification of midlevel mesoscale convective vortices. *Mon. Wea. Rev.,* **129,** 605–637.

Sadler, J. C., 1976: A role of the tropical upper tropospheric trough in early season typhoon development. *Mon. Wea. Rev.,* **104,** 1266–1278.

Schultz, P., 1995: An explicit cloud physics parameterization for operational numerical weather prediction. *Mon. Wea. Rev.,* **123,** 3331–3343.

Simpson, J., E. Ritchie, G. J. Holland, J. Halverson, and S. Stewart, 1997: Mesoscale interactions in tropical cyclone genesis. *Mon. Wea. Rev.,* **125,** 2643–2661.

Sutcliffe, R. C., 1947: A contribution to the problem of development. *Quart. J. Roy. Meteor. Soc.,* **73,** 370–383.

Trenberth, K. E., 1978: On the interpretation of the diagnostic quasi-geostrophic omega equation. *Mon. Wea. Rev.,* **106,** 131–137.

Trier, S. B., and C. A. Davis, 2002: Influence of balanced motions on heavy precipitation within a long-lived convectively generated vortex. *Mon. Wea. Rev.,* **130,** 877–899.

——, ——, and J. D. Tuttle, 2000a: Long-lived mesoconvective vortices and their environment. Part I: Observations from the central United States during the 1998 warm season. *Mon. Wea. Rev.,* **128,** 3376–3395.

——, ——, and W. C. Skamarock, 2000b: Long-lived mesoconvective vortices and their environment. Part II: Induced thermodynamic destabilization in idealized simulations. *Mon. Wea. Rev.,* **128,** 3396–3412.

Zhang, D., and R. A. Anthes, 1982: A high-resolution model of the planetary boundary layer—Sensitivity tests and comparisons with SESAME-79 data. *J. Appl. Meteor.,* **21,** 1594–1609.